Final Draft
of the original manuscript:

Nagorna, T.V.; Kuzmenko, M.O.; Kyzyma, O.A.; Chudoba, D.; Nagornyi, A.V.; Tropin, T.V.; Haramus, V.M.; Jazdzewska, M.; Bulavin, L.A.:
Structural reorganization of fullerene C70 in N-methyl-2-pyrrolidone/toluene mixtures.
In: Journal of Molecular Liquids. Vol. 272 (2018) 948 – 952.
First published online by Elsevier: 23.10.2018

DOI: 10.1016/j.molliq.2018.10.110
https://dx.doi.org/10.1016/j.molliq.2018.10.110

Structural reorganization of fullerene C_{70} in N-methyl-2-pyrrolidone / toluene mixtures

Tetiana V. Nagorna[1,2,*], Maryna O. Kuzmenko[1,2],Olena A. Kyzyma[1,2], Dorota Chudoba[2,3], Anatolii V. Nagornyi[1,2], Timur V. Tropin[2], Vasil M. Garamus[4], Monika Jazdzewska[2,3], Leonid A. Bulavin[1]

[1] Taras Shevchenko National University of Kyiv, Glushkov Prosp. 6, Kiev, 03127 Ukraine

[2] Joint Institute for Nuclear Research, Joliot-Curie St. 6, Dubna, 141980 Russia

[3]Adam Mickiewicz University, Umultowska str. 85, Poznan, 61-614 Poland

[4]Helmholtz-Zentrum Geesthacht: Centre for Materials and Coastal Research, Max-Planck-Str. 1, Geesthacht 21502, Germany

*nagorna@jinr.ru; kuzjamaryna@gmail.com, alyona_kizima@mail.ru, dmn@amu.edu.pl, avnagorny@jinr.ru, ttv@jinr.ru, vasyl.haramus@hzg.de, mojaz@amu.edu.pl, bulavin221@gmail.com

Corresponding author: T.V. Nagorna

e-mail: nagorna@jinr.ru

Joliot-Curie str. 6, Dubna, 141980 Russia

Abstract

The changes in the cluster state of fullerene C_{70} dissolved in N-methyl-2-pyrrolidone/toluene mixture after toluene addition have been studied. In order to measure the wide range of particle sizes, including sub-single-molecule region and respectively large clusters, the Small-Angle X-ray Scattering, Dynamic Light Scattering and UV-Vis spectroscopy were used. The main task was to find out correlation between the fullerene clusterization state and a volume concentration of the second nonpolar solvent. It was observed a common dependence of the structure state of fullerene C_{70} on the polarity of the liquid medium; an increase in toluene content led to further dissolution of existing large agglomerates. The obtained data were analyzed in comparison with the previous results on the inverse colloidal system, C_{70} / toluene / N-methyl-2-pyrrolidone, and also with our semi-empirical calculations and experimental measurements on similar solutions based on fullerene C_{60}.

Keywords: *Fullerenes, Clusterization, Small-Angle X-Ray Scattering, Dynamic Light Scattering, UV -Vis spectroscopy.*

1. Introduction

After discovery of a new allotropic form of carbon - fullerenes, much attention is paid to possibilities of their applications in various fields, including medicine, photoelectronics and optics

[1-5]. In spite of a wide application of fullerene solutions, the processes of their aggregation are still unclear in both weakly polar solvents and their mixtures with polar solvents [6-9]. This problem significantly limits the production of fullerene solutions, including aqueous, with the specified characteristics for the mentioned tasks [10, 11]. It is well-known, that the solubility of fullerenes decreases with increasing polarity of the solvent, and the arising clusterization process is critical and reversible [12]. An exception to this rule is the fullerene solutions in nitrogen-containing solvents, like pyridine or N-methyl-2-pyrrolidone (NMP). Such systems are characterized by a high-rate solubility and formation of large aggregates (~ 100 nm) with time, which is accompanied by a change in the UV-Vis spectrum [13]. This atypical solubility could be a result (or a manifestation) of the formation of donor-acceptor complexes between the fullerenes and NMP molecules [14, 15]. However, the interaction between C_{70} and nitrogen-containing liquids in pure solutions and, in particular, in their mixtures is complicated and still not clear.

In the present work, the processes of fullerene C_{70} cluster formation in the mixture of polar and nonpolar solvents, N-methyl-2-pyrrolidone (dielectric constant $\varepsilon = 32$) and toluene ($\varepsilon = 2.37$), is considered by means of three complementary methods, small-angle X-ray scattering (SAXS), dynamic light scattering (DLS) and UV-Vis spectroscopy. To investigate the influence of the nonpolar solvent on the cluster reorganization processes, toluene was gradually added to the initial system, C_{70}/NMP, in the following proportions: 20 %, 40 %, 60 %, 70 %, 80 % and 90 % by toluene volume. Previous studies on analogous systems based on fullerene C_{60} have shown the critical character of cluster formation, structural changes were observed clearly and sharply when 40 % threshold of toluene volume fraction was exceeded. The critical character of aggregation process is supposedly due to the specific interaction of fullerene with solvent's molecules: the forming charge transfer complexes (CTCs) can serve as stabilizers of the clusters, forming a solvation shell [15-18]. Additionally, we have performed the semi-empirical calculations to clarify the formation of CTCs in the solution and test the influence of low-polar toluene molecules on complexes stability.

2. Materials and Methods

C_{70} fullerene ("Fullerene technologies", purity > 99.5%), toluene and N-methyl-pyrrolidine-2-one (all purchased from "Merck", purity > 99.5%) were used for samples preparation.

The initial C_{70} / NMP solution was intensively stirred for 15 min at the room temperature and further stored for 4 weeks. Initial concentrations were selected individually for each method to comply with the experimental conditions. Further, toluene was added directly to this solution, thus the ternary C_{70} / NMP / toluene systems were obtained. Measurements were performed at different volume fractions of the third component: 0, 20, 40, 60, 70, and 80 % of toluene.

Small-Angle X-ray Scattering experiments were performed at the P12 BioSAXS Beamline at PETRA III ring (EMBL/DESY) in Germany [19]. The sample-to-detector distance, 3.1 m, gave the q-range of $0.04 - 4.6$ nm^{-1} calibrated using silver behenate [20]. Scattering patterns were obtained by a Pilatus 2M pixel detector. The samples were placed into the glass capillary (1 mm of diameter). The temperature was 20±0.1 °C. Twenty consecutive frames (each 0.05 s) comprising the measurement of the sample and buffer were performed. In order to verify that no artifacts as a result of radiation damage occurred, all scattering curves of a recorded dataset were compared to a reference measurement (typically the first exposure) and finally integrated by automated acquisition program [21]. The measurements were carried out immediately after preparation. The sample with 80 % volume fraction of toluene was tested once again in 2 weeks after preparation. The initial concentration 0.61 mg/ml was used. Before and after each sample, a signal from pure buffer was recorded and used for background subtraction. The data were normalized to transmitted beam.

The hydrodynamic size distribution measurements of fullerene aggregates via DLS method were made using the Photocor Compact-Z instrument (Photocor Ltd.). The samples were prepared with the fullerene concentration 0.060±0.001 mg/ml. The solutions were filtered an hour later after mixing and further measured on the instrument. Standard glass vials were used for measurements. The temperature was kept 20±0.05 ^{0}C. Laser with wavelength of 654 nm was used as a light source. The scattered light was collected at the 90° angle. An autocorrelation function of the scattered light intensity was analyzed using the DynaLS software (Alango, Israel). The intensity average (Z-average) hydrodynamic diameter was calculated from the measured diffusivities using the Stokes-Einstein equation [22]. Each measurement was repeated 10 times and the average value is given.

The UV-Vis measurements were carried out immediately after preparation and repeated after 10 days (initial concentration was 0.39 mg/ml). The C_{70} / NMP and C_{70} / NMP / toluene solutions were investigated using the Nanophotometer-P330 UV–Vis spectrophotometer (wavelength range of 200–950 nm). Quartz cells (Hellma Analytics) with optical path of 2 mm were used.

The semi-empirical calculations were performed using the PM6 method [23]. The geometrical structure of several different molecular compositions was thus optimized to reveal the preferential orientations of NMP/toluene molecules in vicinity of fullerene C_{70} surface.

3. Results and discussions

A structural characterization was conducted using the small-angle X-ray scattering method for the initial system C_{70} / NMP and the systems after addition of different fractions of toluene. Experimental data are given on Fig.1. All experimental curves have the typical for polydisperse

systems shape. The series of patterns can be conditionally divided in two groups: systems with a clearly manifested two-level structure (solution without toluene and with 20, 40, and 60 vol. % of toluene, Fig.1a) and systems, which have a large plateau (Fig.1b), a so-called “Guinier region”, responsible for scattering on comparatively large C_{70} clusters, with characteristic sizes above 30 nm. This plateau could be a result of superposition of scattering from several clusters of similar sizes. Scattering contributions from the large aggregates with a fractal structure and relatively small objects were taken into account in the following expression [24, 25]:

$$I(q) = A \cdot \exp(-\frac{q^2 {R_{g1}}^2}{3}) + B \cdot \left[\frac{q}{\left(erf(qR_{g1}/\sqrt{6}) \right)^3} \right]^{-p} \cdot \exp(-\frac{q^2 {R_{g2}}^2}{3}) + C \cdot \exp(-\frac{q^2 {R_{g2}}^2}{3}) + Bkg, \quad (1)$$

where q is the scattering vector; A and C are the forward scattered intensities; B is the constant; p is an exponent; Bkg is the residual incoherent scattering after subtraction of the solvent scattering; R_{g1} and R_{g2} are the radii of gyration of the larger and smaller objects in the system, respectively. Each term in (1) reflects the contribution of the corresponding organization level to an overall diffraction signal, one can see their partial contributions on the example SAXS curve for the pure C_{70} / NMP solution on Fig.1a. The structural parameters were estimated by computing the experimental curves from Fig.1 with a help of eq.(1), they are gathered into a Table.1.

Table 1. Structural parameters of the mixtures with fullerene C_{70} obtained due to approximation by eq. (1).

Toluene content in the mixture, % by volume	Parameters		
	Large sizes		Small sizes
	R_{g1}, nm	p	R_{g2}, nm
0 (the initial solution)	44.0 ± 0.5	4.2 ± 0.1	1.35 ± 0.05
20	–	3.2 ± 0.1	1.45 ± 0.05
40	–	3.4 ± 0.1	1.5 ± 0.1
60	–	4.8 ± 0.2	1.5 ± 0.1
70	30.8 ± 0.5	4.7 ± 0.1	1.9 ± 0.5
80	28.5 ± 0.5	4.8 ± 0.1	–
80 (2 weeks old)	31.5 ± 0.5	4.9 ± 0.1	–

For the first group of curves (20 – 60 % toluene addition), from the well-observed two distinct areas on the SAXS spectra (Fig.1a), we report the coexistence of significant number of small objects together with large agglomerates. The first kind of objects has a characteristic size of R_{g2} = 1.5 ± 0.1 nm. The real size can be estimated using approximation of homogeneous

monodisperse spheres, as $R_g^2 = (3/5)\, R^2$, resulting in $R \sim 1.9 \pm 0.1$ nm. Considering the size of the molecule C_{70} from ref. [26], R_g = 0.7 nm, one can attribute the SAXS signal in the range of $q = 0.5 - 3$ nm^{-1} to the scattering on an ensemble of particles, including the single C_{70} molecules, their dimers, trimers and others. Strictly speaking, the plateau is associated with respectively small polydisperse objects, with their size distribution implying possibility to find C_{70} monomers, dimers etc. It should be noted that analogous R_g value for the initial solution was estimated as R_{g2} = 1.35 ± 0.05 nm. This fact indicates the appearance of slightly larger aggregates among objects of small dimensions after admixing of toluene.

The initial section of the SAXS curves, up to $q = 0.1$ nm^{-1}, is characterized by a power-law behavior, which could indicate a fractal structure of large clusters with sizes extending beyond the typical sensitivity of the method of small-angle scattering. Experimentally obtained exponents for the mixtures with 20, 40 vol. % of toluene are $p = 3.2 \pm 0.1$, $p = 3.4 \pm 0.1$ respectively, thus a structure with the surface fractal behavior is revealed. Their fractal dimensions, $D_{SURF} = 6 - p$, are 2.8 and 2.6. The other type of fractal structure is realized when 60 vol. % of toluene was added to the initial solution. The power-law exponent is $p = 4.8 \pm 0.2$ (see Fig.1a inset). This fact indicates the formation of diffusive surface of large and dense clusters [27]. Comparing the spectra of the C_{70} / NMP and C_{70} / NMP/toluene solutions on Fig.1a, we can conclude that dense clusters with sizes large than 44 nm (R_{g1} for the initial solution) are partially destroyed (mostly on the surface) thus enriching a sub-molecular fullerene fraction. Still, the big clusters are too large to be revealed by SAXS. The final cluster structure correlates with the amount of toluene added to initial solution.

The appearance of the Guinier region for mixtures with toluene content exceeding 70 vol. % may be an indication of the decrease in the sizes of large aggregates. Such a signal can appear as a result of the overlapping of signals from two or more close range of sizes. In this case, the registration of scattering from small aggregates becomes more complicated. Estimation of sizes of large aggregates (R_{g1}) provides the following values: 30.8 ± 0.5 nm, 28.5 ± 0.5 nm, for 70, 80 vol. % of toluene added, and 31.5 ± 0.5 nm for the aged solution 80 vol. %, respectively. Again, the obtained values should be considered only as a lower limit of aggregate sizes because their Guinier regions do not completely appear in the lowest q-range of SAXS curves. Analyzing the changes in power-law intervals for the solutions after addition of toluene, one can notice formation of cluster's structure that is characterized by a higher value of exponent p (see the inset to Fig.1b). Aggregates in the initial solution C_{70} / NMP are described by the exponent, $p = 4.2 \pm 0.1$, typical for objects with diffusive surface [25, 28]. But when toluene is added and its amount in solution and exceeds 70 % concentration the clusters have a structure with a more diffusive surface [27,

28]. Toluene addition leads to a surface dissolving rather than through a volume of large dense aggregates.

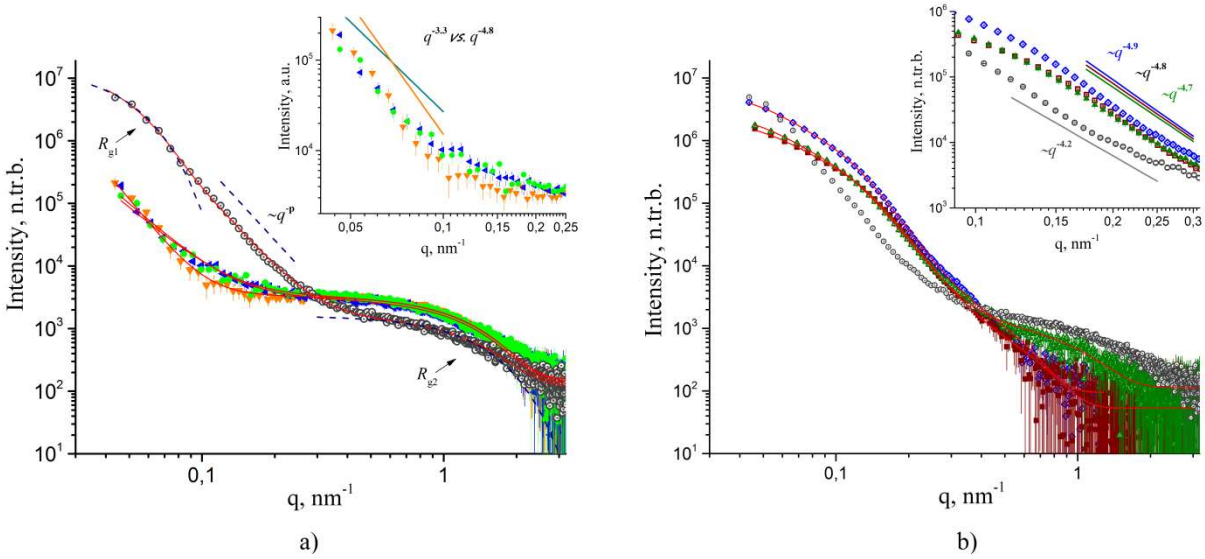

Fig. 1. Experimental SAXS data for the C_{70}/NMP: a) Θ – pure solution (0 % of toluene), ● – with 20 vol. % of toluene, ◀ – 40 vol. % of toluene, ▼ – 60 vol. % of toluene; b) Θ – pure solution, ▲ – 70 vol. % of toluene, ■ – 80 vol. % of toluene, ◊ –80 vol.% of toluene in two weeks after preparation. Red lines are approximations of I(q) using (1). The insets demonstrate the changes in power-law dependencies for certain *q*-intervals when volume fraction of toluene is different. Dashed lines illustrate the contributions of different terms from eq. (1).

The reduction in the size of large aggregates, when toluene fraction reaches and exceeds 70 vol. %, is confirmed by the DLS measurements (Fig.2). All the size-distributions are significantly broad. The results of the treatment show the presence of large aggregates with an average size of about 90 nm in the C_{70} / NMP initial system and reveal some increasing in the cluster's characteristic size when toluene fraction goes up to 60 %. A tendency to destruction of the large aggregates when exceeding 70 % of toluene volume fraction is also observed by DLS. Very small particles, e.g. dimers and trimers, presumably can't be detected by the DLS instrument due to the dominant contribution to quasielastic light scattering of the signal from very large clusters. Two similar groups of aggregates by size (20 and 60 nm) are observed in the system when a volume fraction of toluene reaches a threshold value of 70 %. This probably leads to the observable corresponding plateau at small *q*-values (up to 0.5 nm^{-1}) in the SAXS spectra on Fig.1 b and to suppression of the SAXS signal from small objects at high *q*-values (1-2 nm^{-1}).

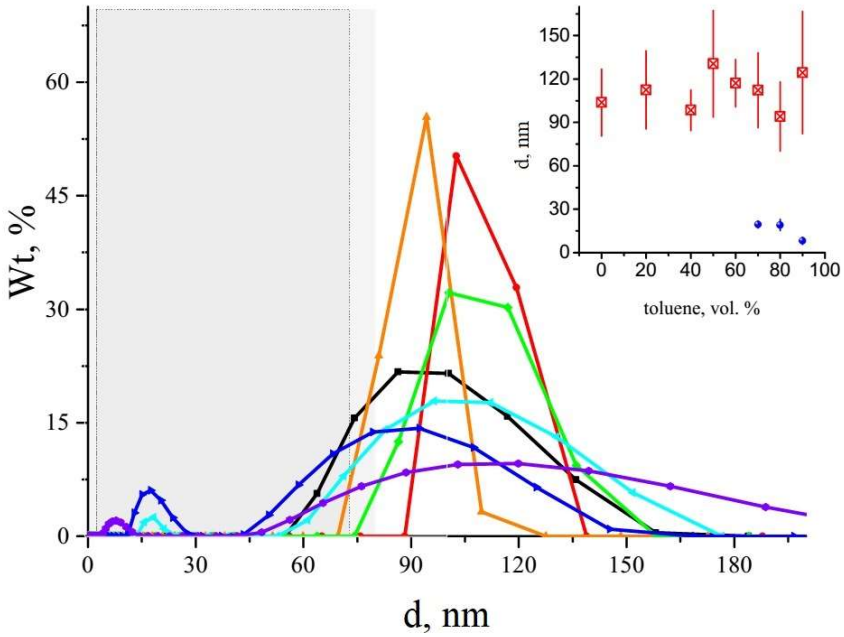

Fig.2. The hydrodynamic size distribution by mass from DLS measurements obtained for C_{70} / NMP / toluene system with different volume fractions of toluene: ● – 0 vol. % (initial solution); ● – 20 vol. %; ● – 40 vol. %; ● – 60 vol. %; ● – 70 vol. %; ● – 80 vol. %; ● – 90 vol. %.. Inset: an average size of the aggregates versus volume fraction of toluene. The dark section outlines an instrumental limits of SAXS to cover a size experimentally.

The UV-Vis spectra of the C_{70} / NMP solution and the ternary system C_{70} / NMP / toluene are given in Fig.3. It can be seen that the intensity decreases for the system with 20 % of toluene. Further increase in the amount of toluene leads to a hyperchromic effect. The change in the extinction coefficient is given in the inset to the Fig.3. The UV-Vis data do not reveal any critical behavior at 70 % of toluene volume fraction. The smoothed absorption spectrum of the system in 10 days after preparation indicates a significant presence of NMP molecules in the shell of C_{70} aggregates even with a small fraction of NMP (~ 20%) in the mixture, because such smoothed spectrum is characteristic for the pure fullerene solution in NMP [29, 30].

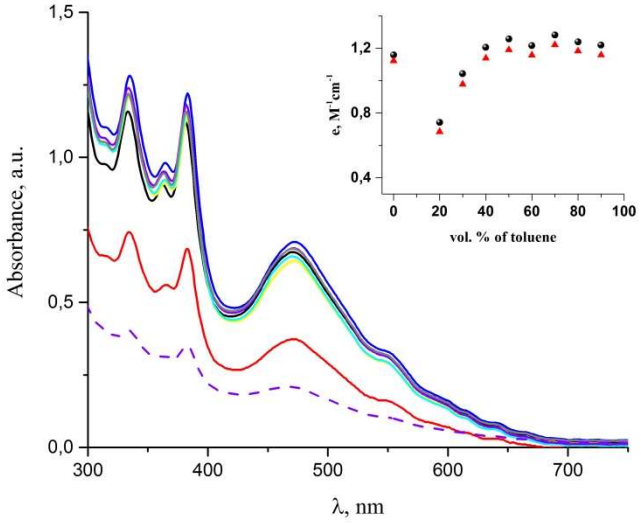

Fig. 3. UV-Vis spectra of the C_{70} NMP solution with various ratio of toluene: ▬ – initial solution; ▬ – 20%; ▬ – 40%; ▬ – 60%; ▬ – 70%; ▬ – 80%; ▬ – 90%; - - – 80% in 10 days. The inset demonstrates dependence of the extinction coefficient at two different wavelengths of 334 nm (●) and 383 nm (▲) versus the toluene volume fraction in the mixture. The spectra are scaled to the unit fullerene concentration.

Some notion on the mechanism of interaction between fullerene C_{70} and solvent molecules (NMP, toluene), and the changes on dissolution of C_{70} / NMP mixture by toluene can be obtained from *ab initio* calculations. The geometrical structure of the following molecular systems: C_{70}-NMP, C_{70}-toluene, C_{70}-2toluene C_{70}-2NMP, C_{70}-2NMP/toluene was optimized using the PM6 method. The obtained structures are presented on Fig.4. For single or two NMP molecules (C_{70}-NMP, C_{70}-2NMP) we obtain the formation of C_{70}-NMP CTCs, with the NMP molecule as the donor of electron and C_{70} as acceptor. As in the case of C_{60}-NMP CTC [31], NMP orients its oxygen atom towards the middle of the plane of the aromatic hexagon of the C_{70} molecule. The distance between oxygen and plane is 2.99 Å. Addition of the second NMP molecule (C_{70}-2NMP on Fig.4) does not qualitatively change the situation. The second NMP molecule is negligibly farther from the C_{70} molecule (3.03 Å). In a similar, but less pronounced way, toluene is interacting with C_{70} (Fig.4). The aromatic hexagon rings of C_{70} and toluene are parallel, the plane-to-lane distance is 3.7 Å.

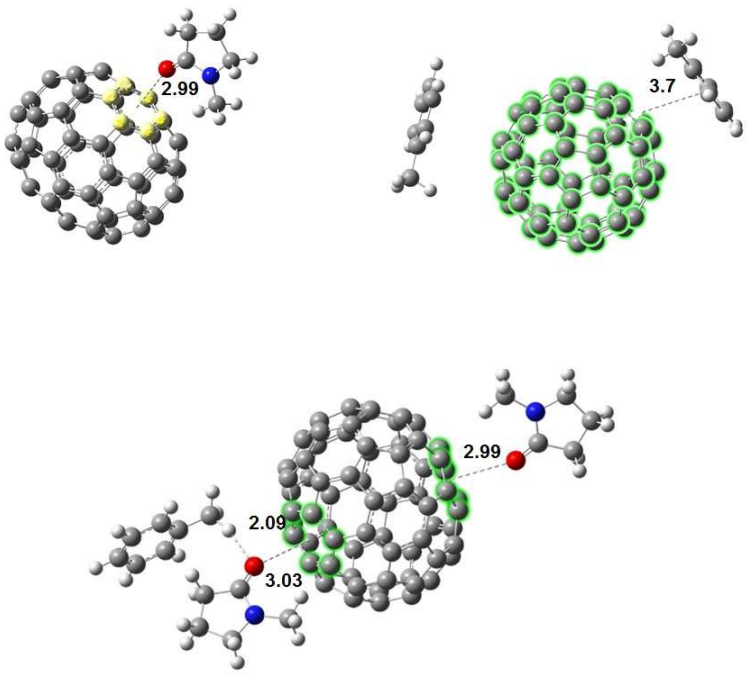

Fig.4. Optimized geometrical structures of the molecular complexes composed of a single C_{70} with NMP/toluene molecules. The C_{70}-NMP, C_{70}-2toluene, C_{70}-2NMP/toluene complexes are demonstrated. The highlighted hexagons on fullerene surface correspond to the closest to respective molecule plane.

Further, the calculations show, that addition of toluene molecule to the C_{70}-2NMP system does not significantly change the respective orientations and distances between nitrogen-containing molecules and fullerene. The hydrogen of methyl group of toluene approaches oxygen atom of the NMP molecule with the hydrogen bonding [32] length of 2.09 Å. We attribute the results of these calculations as an additional confirmation of the fact, that only excessive amounts of toluene are capable of unbinding the C_{70}-NMP CTCs that were formed in the pure C_{70}/NMP solution.

4. Conclusions

Using the methods of small-angle X-ray scattering and dynamic light scattering we report the big aggregates with a size ~ 90 nm in all systems studied. The presence of small aggregates in the C_{70} / NMP / toluene system with sizes of about 30 nm for volume fraction of toluene above 70 % was detected. At the same time, the spectra obtained via UV-Vis spectroscopy methods do not exhibit criticality in the given range. This fact indicates that the changes in the absorption spectra with a change of solvent polarity in the composition of the mixture are first of all due to the solvation effects of fullerene C_{70} by toluene.

In spite of the fact that toluene solvation processes are already observed at small fractions of the nonpolar component, aggregate destruction occurs only when the toluene fraction is more than 70%. Thus, the effect of selective solvation is observed in the mixture, when the ratio of solvents in the shell around the fullerene shifts in favor of NMP and does not coincide with the ratio of solvents in the volume of the system. This is also supported by the semi-empirical calculations that show the tendency of C_{70}-NMP CTCs formation and their stability in presence of the toluene molecule. For the same reason effect of smoothing in the UV-Vis spectra with time is observed. As a result, the reorganization of clusters is observed when the ratio of solvents is shifted towards the lower polarity. The presence of NMP molecules in the solvate shell does not allow further reorganization of the fullerene clusters in the mixture even with a high proportion of toluene (80%) and, according to the SAXS data, the system remains stable for at least a month.

Acknowledgements

We gratefully acknowledge Clement Blanchet for help during SAXS experiment at the P12 BioSAXS beamline (EMBL/DESY, PETRA III).

References

1. Guan M., Ge J., Wu J., Zhang G., Chen D., Zhang W. et al. Fullerene/photosensitizer nanovesicles as highly efficient and clearable phototheranostics with enhanced tumor accumulation for cancer therapy. J. Biomaterials. 2016; 103:75–85. http://dx.doi.org/10.1016/j.biomaterials.2016.06.023

2. Prylutska S.V., Burlaka A.P., Klymenko P.P., Grynyuk I. I., Prylutskyy Yu.I., Schütze Ch. et al., Using water-soluble C_{60} fullerenes in anticancer therapy. Cancer Nanotechnol. 2011; 2(1-6): 105–110. http://dx.doi.org/10.1007/s12645-011-0020-x

3. Wang L., Solvated fullerenes, a new class of carbon materials suitable for high-pressure studies: A review. J. Phys. Chem. Solids. 2015;84:85–95. http://dx.doi.org/10.1016/j.jpcs.2014.06.007

4. Xing M., Wang R., Yu J., Application of fullerene C_{60} nano-oil for performance enhancement of domestic refrigerator compressors. Int. J. Refrigeration. 2014;40:398–403. http://dx.doi.org/10.1016/j.ijrefrig.2013.12.004

5. Afreen S., Muthoosamy K., Manickam S., Hashim U. Functionalized fullerene (C_{60}) as a potential nanomediator in the fabrication of highly sensitive biosensors. Biosens. Bioelectron. 2015;63:354–364. http://dx.doi.org/10.1016/j.bios.2014.07.044

6. Tropin T.V., Avdeev M.V., Kyzyma O.A., Aksenov V.L., Nucleation theory models for describing kinetics of cluster growth in C_{60}/NMP solutions. Phys. Status Solidi B. 2010;247(11-12):3022–3025. http://dx.doi.org/10.1002/pssb.201000119

7. Aksenov V. L., Tropin T.V., Kyzyma O.A., Avdeev M.V., Korobov M.V., Rosta L., Formation of C_{60} fullerene clusters in nitrogen-containing solvents. Phys. Solid State.2010;52:1059–1062. http://dx.doi.org/10.1134/S1063783410050367

8. Kyzyma O.A., Korobov M.V., Avdeev M.V., Garamus V.M., Snegir S.V., Petrenko V.I., Aksenov V.L., Bulavin L.A. Aggregate development in C_{60}/N-metyl-2-pyrrolidone solution and its mixture with water as revealed by extraction and mass spectroscopy. Chem. Phys. Lett. 2010;493:103–106. http://dx.doi.org/10.1016/j.cplett.2010.04.076

9. Nagorna T.V., Kyzyma O.A., Chudoba D., Nagornyi A.V. Temporal solvatochromic effect in ternary C_{70}/toluene/N-methyl-pyrrolidine-2-one solution. J. Mol. Liq. 2017;235:111–114. http://dx.doi.org/10.1016/j.molliq.2016.12.017

10. Korolovych V.F., Nedyak S.P., Moroz K.O., Prylutskyy Yu.I., Scharff P., Ritter U. Compressibility of Water Containing Single-Walled Carbon Nanotubes. Fullerenes, Nanotubes and Carbon Nonstructures. 2013; 21:24-30. http://dx.doi.org/10.1080/1536383X.2011.574301

11. Korolovych V.F., Bulavin L.A., Prylutskyy Yu.I., Khrapatiy S.V., Tsierkezos N.G.,·Ritter U. Influence of Single-Walled Carbon Nanotubes on Thermal Expansion of Water. Int J Thermophys. 2014; 35(1):19-31. http://dx.doi.org/10.1007/s10765-013-1552-6

12. Mchedlov-Petrossyan N.O., Kamneva N.N., Al-Shuuchi Y.T.M., Marynin A.I., Shekhovtsov S.V., The peculiar behavior of fullerene C_{60} in mixtures of 'good' and polar solvents: colloidal particles in the toluene–methanol mixtures and some other systems, Colloids Surf. A. 2016;509:631–637. http://dx.doi.org/10.1016%2Fj.colsurfa.2016.09.045

13. Tropin T.V., Kyrey T.O., Kyzyma O.A., Feoktistov A.V., Avdeev M.V., Bulavin L.A., Rosta L., Aksenov V.L. Experimental investigation of C_{60}/NMP/toluene solutions by UV-Vis spectroscopy and small-angle neutron scattering. J. Synch. Investig. 2013;7:1–4. http://dx.doi.org/10.1134/S1027451013010199

14. Kyzyma O.A., Korobov M.V., Avdeev M.V., Garamus V.M., Petrenko V.I., Aksenov V.L. , Bulavin L.A. Solvatochromism and fullerene cluster formation in C_{60}/N-methyl-2-pyrrolidone. Fullerenes, Nanotubes and Carbon Nanostructures. 2010;18:458–461. http://dx.doi.org/10.1080/1536383X.2010.487778

15. Yevlampieva N.P., Biryulin Yu.F., Melenevskaja E.Yu., Zgonnik V.N., Rjumtsev E.I. Aggregation of fullerene C_{60} in N-methylpyrrolidone . Colloids Surf. A. 2002;209(2-3):167–171. http://dx.doi.org/10.1016/S0927-7757(02)00177-2

16. Avdeev M.V., Aksenov V.L., Tropin T.V. Models of cluster formation in solutions of fullerenes, Russ. J. Phys. Chem. A. 2010;84:1273−1283. http://dx.doi.org/10.1134/S0036024410080017

17. Mrzel A., Mertelj A., Omerzu A., Cyopic M., Mihailovic D. Investigation of encapsulation and solvatochromism of fullerenes in binary solvent mixtures . J. Phys. Chem. B. 1999;103(51):11256–11260. http://dx.doi.org/10.1021/jp992637e

18. Baibarac M., Mihut L., Preda N., Baltog I., Mevellec J.Y., Lefrant S. Surface-enhanced Raman scattering studies on C_{60} fullerene self-assemblies. Carbon. 2005;43(1):1–9. http://dx.doi.org/10.1016/j.carbon.2004.08.020

19. Blanchet C.E., Spilotros A., Schwemmer F., Graewert M.A., Kikhney A., Jeffries C.M. et al. Versatile sample environments and automation for biological solution X-ray scattering experiments at the P12 beamline (PETRA III, DESY). J. Appl. Crystallogr. 2015;48:433–443. http://dx.doi.org/10.1107/S160057671500254x

20. Blanton T.N., Barnes C.L., Lelental M. Preparation of silver behenate coatings to provide low- to mid-angle diffraction calibration . J. Appl. Crystallogr. 2000;33:172–173. http://dx.doi.org/10.1107/S0021889899012388

21. Franke D., Kikhney A.G., Svergun D.I. Automated acquisition and analysis of small angle X-ray scattering data. Nucl. Instrum. Methods Phys. Res. A. 2012;689:52–59. http://dx.doi.org/10.1016/j.nima.2012.06.008

22. Stetefeld J., McKenna S.A., Patel T.R. Dynamic light scattering: a practical guide and applications in biomedical sciences, Biophys. Rev., 2016; 8:409–427. http://dx.doi.org/10.1007/s12551-016-0218-6

23. Stewart J. J. P. Optimization of parameters for semiempirical methods. V: Modification of NDDO approximations and application to 70 elements. J. Mol. Model. 2007;13(12):1173–1213. http://dx.doi.org/10.1007/s00894-007-0233-4

24. Beaucage G. Small-Angle scattering from polymeric mass fractals of arbitrary mass-fractal dimension. J. Appl. Crystallogr. 1996;29:134–149. http://dx.doi.org/10.1107/S0021889895011605

25. Avdeev M.V., Tomchuk O.V., Ivankov O.I., Alexenskii A.E., Dideikin A.T., Vul A.Ya. On the structure of concentrated detonation nanodiamond hydrosols with a positive ζ potential:

Analysis of small-angle neutron scattering. Chem. Phys. Lett. 2016;658:58–62. http://dx.doi.org/10.1016/j.cplett.2016.06.010

26. Nikolaev A.V., Dennis T.J.S., Prassides K., Soper A.K., Molecular structure of the C_{70} fullerene, Chem. Phys. Lett. 1994;223(3):143–148. http://dx.doi.org/10.1016/0009-2614(94)00432-3

27. Beaucage G. Approximations Leading to a Unified Exponential/Power-Law Approach to Small-Angle Scattering. J. Appl. Crystallogr. 1995;28:717–728. http://dx.doi.org/10.1107/S0021889895005292

28. Tomchuk O.V., Bulavin L.A., Aksenov V.L., Garamus V.M., Ivankov O.I., Vul' A.Ya. et al. Small-angle scattering from polydisperse particles with diffusive surface. J. Appl. Crystallogr. 2014;47:642–653. http://dx.doi.org/10.1107/S1600576714001216

29. Tropin T.V., Jargalan N., Avdeev M.V., Kyzyma O.A., Eremin R.A., Sangaa D. et al. Kinetics of cluster growth in polar solutions of fullerene: Experimental and theoretical study of C_{60}/NMP solution, J. Mol. Liq. 2012;175:4–11. http://dx.doi.org/10.1016/j.molliq.2012.08.003

30. Kyzyma O.A., Bulavin L.A., Aksenov V.L., Avdeev M.V., Tropin T.V., Korobov M.V. et al. Aggregation in C_{60}/NMP, C_{60}/NMP/water and C_{60}/NMP/toluene mixtures. Fullerenes, Nanotubes and Carbon Nonstructures. 2008;16:610–615. http://dx.doi.org/10.1080/15363830802312982

31. Karpenko O.B., Trachevskij V.V., Filonenko O.V., Lobanov V.V., Avdeev M.V., Tropin T.V., Kyzyma O.A., Snegir S.V. NMR study of non-equilibrium state of fullerene C_{60} in n-methyl-2-pyrrolidone. Ukr. J. Phys. 2012;57(8):860-863. http://archive.ujp.bitp.kiev.ua/files/journals/57/8/570810p.pdf

32. Taylor R., Kennard O. Molecular structures of nucleosides and nucleotides. 2. Orthogonal coordinates for standard nucleic acid base residues, J. Am. Chem. Soc., 1982;104 (11):3209–3212. http://dx.doi.org/10.1021/ja00375a046